ISCIT 2004

International Symposium on Communications
and Information Technologies 2004 (ISCIT 2004)
Sapporo, Japan, October 26- 29, 2004

Convergence Analysis of MultiModulus-Based Blind Equalization Algorithms

Wen-Chun Chien and Jenq-Tay Yuan

Department of Electronic Engineering, Fu Jen Catholic University

Taipei 24205, Taiwan, R.O.C.

E-mail: yuan@ee.fju.edu.tw

Abstract

This work proposes a new blind equalization algorithm referred to herein as the multimodulus stop-and-go decision-directed algorithm (MSG-DDA), by combining the advantages of both an existing multimodulus algorithm (MMA) and a well-known stop-and-go algorithm (SGA). The dynamic convergence properties of the MSG-DDA and the MMA for blind equalization are then mathematically analyzed using a conditional Gaussian approximation. The results verify that the MSG-DDA substantially outperforms both the MMA and SGA.

I. INTRODUCTION

Adaptive channel equalization without a training sequence is known as blind equalization [1] – [7]. The major advantage of such a technique is that no training sequence is required to start or restart the system when the communication unexpectedly breaks down. Figure 1 illustrates an equivalent baseband model with a channel impulse response of $h(n)$. The channel input, additive white Gaussian noise, and equalizer input are denoted by $a(n)$, $v(n)$, and $x(n)$, respectively. The data symbols transmitted, $\{a(n)\}$, are assumed to consist of stationary independently and identically distributed (i.i.d.), real or complex non-Gaussian random variables. The channel is possibly a nonminimum phase linear time-invariant filter. The equalizer input, $x(n)=\sum_{i=0}^{N-1} h(i)a(n-i)+v(n)$, which is assumed to be stationary, is then sent to a tap-delay-line blind equalizer intended to equalize the distortion caused by inter-symbol interference (ISI) without a training signal. The output of the blind equalizer $z(n)=\mathbf{c}^H(n)\mathbf{x}(n)$ can be used to recover the transmitted data symbols, $a(n)$, where $\mathbf{x}^T(n)=[x(n+L),...,x(n-L)]$ is the equalizer input vector, and $\mathbf{c}^T(n)=[c_{-L}(n),...,c_L(n)]$ is the equalizer tap vector with the number of equalizer taps $N = (2L+1)$.

In this work, the dynamic convergence of an existing multimodulus algorithm (MMA) and a proposed multimodulus stop-and-go decision-directed algorithm (MSG-DDA), which combines the MMA and the SGA for blind equalization, is analyzed. The theoretical results demonstrate that the proposed algorithm substantially outperforms the MMA and SGA. The convergence analysis is facilitated by a transformation to orthogonalize (whiten) the equalizer input data vector $x(n)$, as follows. The input covariance matrix $\mathbf{R}=E\{\mathbf{x}(n)\mathbf{x}^H(n)\}$ can be decomposed as $\mathbf{R}=\mathbf{U}^H\mathbf{\Lambda}\,\mathbf{U}$, where U is a unitary matrix and $\mathbf{\Lambda}=diag\{\lambda_1,\lambda_2,...,\lambda_N\}$ where λ_i are the eigenvalues of $\boldsymbol{R}$. Notably, $\{x(n)\}$ are assumed to be stationary, so the input covariance matrix $\boldsymbol{R}$ is independent of the time n. The transformed tap weight vector and the transformed equalizer input vector are $\mathbf{w}(n)=\mathbf{U}\mathbf{c}(n)$ and $\mathbf{y}(n)=\mathbf{U}\mathbf{x}(n)$, respectively. Accordingly, the output of the equalizer can also be expressed as $z(n)=\mathbf{w}^H(n)\mathbf{y}(n)=z_R(n)+jz_I(n)$ in the transformed domain, where $z_R(n)$ and $z_I(n)$ are the real and imaginary parts of the equalizer output, respectively. The MMA, the SGA and the MSG-DDA are briefly described as follows.

A. MultiModulus algorithm (MMA)

The constant modulus algorithm (CMA) is one of the most widely used blind equalization algorithms. The CMA cost function is invariant to a phase rotation in the constellation, so consequently, the equalizer output signal constellation suffers from an arbitrary phase rotation. Oh and Chin [1], and Yang, Werner, and Dumont [2] proposed a modified CMA called the multimodulus algorithm (MMA), whose cost function is

$$J_{MMA}=J_R(n)+J_I(n)=E\{[z_R^2(n)-R_{2,R}]^2\}+E\{[z_I^2(n)-R_{2,I}]^2\} \quad (1)$$

where $R_{2,R}$ and $R_{2,I}$ are given by $R_{2,R}=\frac{E\{a_R^4(n)\}}{E\{a_R^2(n)\}}$ and $R_{2,I}=\frac{E\{a_I^4(n)\}}{E\{a_I^2(n)\}}$, in which $a_R(n)$ and $a_I(n)$ denote the real and imaginary parts of $a(n)$, respectively. Decomposing the cost function of the MMA into the real and imaginary parts thus allows both the *modulus* and the *phase* of the equalizer output to be considered; therefore, joint *blind equalization* and *carrier phase recovery* may be simultaneously accomplished, eliminating the need for a rotator to perform separate constellation phase recovery in steady-state operation [1] – [3]. Analysis results in [3]

indicate that the MMA alone is able to remove inter-symbol interference (ISI) and simultaneously correct the phase error, because it implicitly incorporates a phase-tracking loop, which automatically recovers carrier phase. Various computer simulations demonstrate that the MMA outperforms the CMA, and both algorithms require an almost identical computational cost. The transformed tap-weight vector of the MMA is updated using the stochastic gradient descent algorithm

$$\mathbf{w}(n+1) = \mathbf{w}(n) - \mu \cdot e_m^*(n) \cdot \mathbf{y}(n) \qquad (2)$$

where $e_m(n) = e_{m,R}(n) + j \cdot e_{m,I}(n)$ in which

$e_{m,R}(n) = z_R(n) \cdot (z_R^2(n) - R_{2,R})$ and $e_{m,I}(n) = z_I(n) \cdot (z_I^2(n) - R_{2,I})$.

Notably, $R_{2,R} = R_{2,I} = R_2$ for QAM systems with a symmetric constellation and their values can be computed to be 1.0, 8.2, and 37 for 4-QAM, 16-QAM, and 64-QAM, respectively.

B. Stop-And-Go Algorithm (SGA)

The stop-and-go algorithm [4] employs the decision-directed (*DD*) error signal given by $e_{dd}(n) = e_{dd,R}(n) + j e_{dd,I}(n) = z(n) - Q[z(n)]$ and adapts the coefficients when the reliability of the decision device is judged to be adequate, where $Q(.)$ is the decision function. This algorithm utilizes the Godard (or Sato) error to control the adaptation of the DD algorithm and has been demonstrated to improve the blind convergence characteristics of the conventional algorithm [5]. The SGA utilizing the Sato-like error has been analyzed in [7].

C. MultiModulus Stop-and-Go Decision-Directed Algorithm (MSG-DDA)

An algorithm, *MSG-DDA*, is now proposed by combining the *MMA* with the SGA. The *MSG-DDA* adapts the coefficients only when the sign of the *DD* error, $e_{dd}(n)$, is the same as that of the MMA error, $e_m(n)$. The real and imaginary parts of the error signal for the *MSG-DDA* are given by

$$e_{msg,\gamma}(n) = f_\gamma(n) e_{dd,\gamma}(n), \text{ for } \gamma = R, I \quad , \quad \text{where}$$

$$f_R(n) = \begin{cases} 1 & \text{if } \operatorname{sgn}\{e_{dd,R}(n)\} = \operatorname{sgn}\{e_{m,R}(n)\} \\ 0 & \text{otherwise} \end{cases} \quad \text{and}$$

$$f_I(n) = \begin{cases} 1 & \text{if } \operatorname{sgn}\{e_{dd,I}(n)\} = \operatorname{sgn}\{e_{m,I}(n)\} \\ 0 & \text{otherwise} \end{cases}$$

are two binary-valued flags that determine whether coefficients will be adapted. Replacing $e_m(n)$ in (2) by $e_{msg}(n) = e_{msg,R}(n) + j e_{msg,I}(n)$ and separately considering the real and imaginary parts allows (2) to be given by

$$\operatorname{Re}\{\mathbf{w}(n+1)\} + j \operatorname{Im}\{\mathbf{w}(n+1)\} = \operatorname{Re}\{\mathbf{w}(n)\} + j \operatorname{Im}\{\mathbf{w}(n)\} - \mu \cdot \{e_{msg,R}(n) - j e_{msg,I}(n)\} \cdot [\mathbf{y}_R(n) + j \mathbf{y}_I(n)]$$

Algebraic manipulation yields the following MSG-DDA:

$$\operatorname{Re}\{\mathbf{w}(n+1)\} = \operatorname{Re}\{\mathbf{w}(n)\} - \mu \cdot [f_R(n) \cdot e_{dd,R}(n) \cdot \mathbf{y}_R(n) + f_I(n) \cdot e_{dd,I}(n) \cdot \mathbf{y}_I(n)] \text{ and}$$

$$\operatorname{Im}\{\mathbf{w}(n+1)\} = \operatorname{Im}\{\mathbf{w}(n)\} - \mu \cdot [f_R(n) \cdot e_{dd,R}(n) \cdot \mathbf{y}_I(n) - f_I(n) \cdot e_{dd,I}(n) \cdot \mathbf{y}_R(n)]$$

Computer simulations indicate that the MSG-DDA can markedly outperform both the MMA and the SGA. To the authors' knowledge, the MSG-DDA is probably one of the best T-spaced blind equalizers in terms of both the rate of convergence and the steady-state mean squared error (*MSE*), as demonstrated by computer simulations. These results motivate the authors to analyze mathematically the dynamic convergence properties of the MSG-DDA for blind equalization. The analytic expressions for the evolution of the MSE trajectory confirm that the proposed algorithm indeed substantially outperforms the MMA and the SGA. For the 16-QAM constellations with the transmitted symbol levels ± 1 and ± 3, the real part of the error signal associated the *MSG-DDA*, for example, can be computed as $e_{msg,R}(n) = 3 + z_R(n)$ when $z_R(n) \le -3$, because when both $z_R(n) \le -3$ and $\operatorname{sgn}[z_R(n)(z_R^2(n) - 8.2)] = \operatorname{sgn}[e_{m,R}(n)] = \operatorname{sgn}[e_{dd,R}(n)] = \operatorname{sgn}[3 + z_R(n)]$ [such that the sign of the *DD* error coincides with the MMA error] are satisfied, that $-\sqrt{8.2} \le z_R(n) \le -2$ or $z_R(n) \le -3$ can be readily computed. Either $-\sqrt{8.2} \le z_R(n) \le -2$ or $z_R(n) \le -3$ in turn yields $e_{msg,R}(n) = e_{dd,R}(n) = z(n) - Q[z(n)] = z_R(n) + 3 = s[z_R(n)]$ as given in Table I. Other results denoted by $s(\cdot)$ can be similarly obtained, and are summarized in Table I, from which $e_{msg,R}(n)$ can be written as $e_{msg,R}(n) \equiv s[z_R(n)]$. The imaginary part of the error signal for the *MSG-DDA*, $e_{msg,I}(n)$, can also be obtained by applying the same function $s(\cdot)$, depicted in Table I, except that $z_R(n)$ has been replaced by $z_I(n)$, such that $e_{msg,I}(n) \equiv s[z_I(n)]$.

II. CONVERGENCE ANALYSIS

The primary objective of this work is to derive an expression for the output *MSE* trajectory for the system under consideration for analysis purposes. The output *MSE* is given by

$$E\{|\varepsilon(n)|^2\} = E\{|d(n) - z(n)|^2\}$$

$$= E\{|d(n)|^2\} + E\{|z(n)|^2\} - 2\operatorname{Re}\{E[d^*(n)z(n)]\} \qquad (3)$$

where $d(n) = a(n - D)$ and D is the overall propagation delay of the channel and the equalizer. As in [6], the following assumptions and approximations are employed in this paper for the convergence analysis to overcome the problems introduced by the nonlinearity of the blind equalization algorithms: (a) the real and imaginary parts of the data symbols transmitted, $\{a(n)\}$, derived from a

QAM constellation are i.i.d. non-Gaussian random variables; (b) the equalizer input vector **x(n)** conditioned on *a(n)* is a complex Gaussian random vector. Accordingly, the equalizer output, *z(n)*, conditioned on *a(n)* and **w(n)** is also a complex Gaussian random variable; (c) the components of the transformed tap weight vector **w(n)** are uncorrelated; (d) the tap weight vector **c(n)** is independent of the equalizer input vector, **x(n)**.

Based on assumptions (a) and (d), the output *MSE* in (3) can be expressed as

$$E\{|\varepsilon(n)|^2\} = E\{|d(n)|^2\}[1 - 2\,\mathrm{Re}\{\mathbf{M}^H(n)\boldsymbol{\eta}\}] + \sum_{k=0}^{N-1}\Gamma_k(n)\lambda_k \quad (4)$$

where $\Gamma_k(n) = E\{|w_k(n)|^2\}$, $M_k(n) = E\{w_k(n)\}$, $k = 0, 1, ..., N-1$; $\mathbf{M}^T(n) = [M_0(n), M_1(n), ..., M_{N-1}(n)]$ and $\boldsymbol{\eta} = \mathbf{U}\bar{\mathbf{h}}$ is the transformed channel impulse response vector where $\bar{\mathbf{h}}$ can be derived to be $\bar{\mathbf{h}} = [h(D), h(D-1), ..., h(D-N+1)]^T$. Notably, in computing (4), $E\{|d(n)|^2\}$, $\boldsymbol{\eta}$, and λ_k are fixed values for stationary data constellations and for a particular channel impulse response, whereas both $M_k(n)$ and $\Gamma_k(n)$ are time-varying. For both the MMA and the MSG-DDA, the recursive relations for the first- and second-order moments of the equalizer tap coefficients $M_k(n)$ and $\Gamma_k(n)$ can be derived by first setting $e_m(n) = e(n)$ in (2) such that

$$\mathbf{w}(n+1) = \mathbf{w}(n) - \mu \cdot e^*(n) \cdot \mathbf{y}(n) \quad (5)$$

Based on assumption (b), $M_k(n)$ and $\Gamma_k(n)$ are required to compute $E\{|\varepsilon(n)|^2\}$ in (4) as a function of n, which can be derived by taking the expectations on both sides of (5) and the expectations of the square of the moduli thereof, respectively, as follows

$$M_k(n+1) = M_k(n) - \mu E\{y_k(n)e^*(n)\} \quad (6)$$

$$\Gamma_k(n+1) = \Gamma_k(n) - 2\mu \cdot E\{\mathrm{Re}[w_k^*(n) \cdot y_k(n) \cdot e^*(n)]\} + \mu^2 E\{|y_k(n)|^2 \cdot |e^*(n)|^2\} \quad (7)$$

where *e(n)* is set to be $e_m(n)$ and $e_{mvg}(n) = s[z_R(n)] + js[z_I(n)]$, respectively, when the MMA and the MSG-DDA are considered. Therefore, (6) and (7) together with the output MSE given by (4) describe completely the evolution of the MSE, with the channel impulse response and the data constellation statistics determining the specific characteristics.

The following results based on assumption (d) are also applied in deriving the transient behavior of the MSE.

$E\{\mathbf{y}(n) \mid d(n)\} = d(n)\mathbf{U}\bar{\mathbf{h}} = d(n)\boldsymbol{\eta} = \boldsymbol{\mu}_y(n)$;

$\mathbf{C} = Cov\{\mathbf{y}(n), \mathbf{y}(n) \mid d(n)\} = \boldsymbol{\Lambda} - E\{|d(n)|^2\} \cdot \boldsymbol{\eta} \cdot \boldsymbol{\eta}^H$;

$E\{z(n) \mid d(n), \mathbf{w}(n)\} \cong E\{z(n) \mid d(n)\} = d(n)\mathbf{M}^H(n)\boldsymbol{\eta} = d(n)p(n) = \mu_z(n)$;

$Cov\{\mathbf{y}(n), z(n) \mid d(n), \mathbf{w}(n)\} = \mathbf{C}\mathbf{w}(n) = \boldsymbol{\Phi}(n)$.

The equalizer input *y(n)* conditioned on *d(n)* is approximately Gaussian so the equalizer output *z(n)* conditioned on both *d(n)* and the equalizer tap vector **w(n)** is also approximately Gaussian. Hence, let *y(n)* and *z(n)* be jointly Gaussian random variables with means and variances given by $E\{y(n) \mid d(n), \mathbf{w}(n)\} = \mu_y(n)$, $E\{z(n) \mid d(n), \mathbf{w}(n)\} = \mu_z(n)$, $VAR\{y(n) \mid d(n), \mathbf{w}(n)\} = \sigma_y^2(n)$ and $VAR\{z(n) \mid d(n), \mathbf{w}(n)\} = \sigma_z^2(n)$ such that the conditional mean and variance of *y(n)*, given *z(n)*, are

$$E\{\mathbf{y}(n) \mid z(n)\} = \boldsymbol{\mu}_y(n) + \frac{\boldsymbol{\Phi}(n)}{\sigma_z^2(n)}[z(n) - \mu_z(n)] \quad \text{and}$$

$$VAR\{\mathbf{y}(n) \mid z(n)\} = \boldsymbol{\sigma}_y^2(n) - \frac{|\boldsymbol{\Phi}(n)|^2}{\sigma_z^2(n)},$$ where each element of $|\boldsymbol{\Phi}(n)|^2$ is the magnitude square of each corresponding element of $\boldsymbol{\Phi}(n)$.

The output *MSE* in (4) is computed using (6) and (7) by first computing $E\{y_k(n)e^*(n)\}$, $E\{w_k^*(n)y_k(n)e^*(n)\}$, and $E\{|y_k(n)|^2 \cdot |e^*(n)|^2\}$. $E\{y_k(n)e^*(n)\}$, where $e(n) \equiv e[z(n)]$, is determined by first computing

$$E\{\mathbf{y}(n)e^*(n) \mid d(n), \mathbf{w}(n)\}$$

$$= E\{e^*(n) \cdot E[\mathbf{y}(n) \mid z(n)] \mid d(n), \mathbf{w}(n)\}$$

$$= E\left\{e^*(n) \cdot \left\{\boldsymbol{\mu}_y(n) + \frac{\boldsymbol{\Phi}(n)}{\sigma_z^2(n)}[z(n) - \mu_z(n)]\right\} \mid d(n), \mathbf{w}(n)\right\}$$

$$= \boldsymbol{\mu}_y(n) \cdot \theta_1^*(n) + \frac{\boldsymbol{\Phi}(n)}{\sigma_z^2(n)} \cdot \theta_3(n) - \frac{\boldsymbol{\Phi}(n) \cdot \mu_z(n)}{\sigma_z^2(n)} \cdot \theta_1^*(n)$$, where

$\theta_1^*(n) = E\{e^*(n) \mid d(n), \mathbf{w}(n)\}$ and

$\theta_3(n) = E\{z(n)e^*(n) \mid d(n), \mathbf{w}(n)\}$. Averaging $E\{\mathbf{y}(n)e^*(n) \mid d(n), \mathbf{w}(n)\}$ over the conditioning variables yields $E\{\mathbf{y}(n)e^*(n)\} = E[E\{\mathbf{y}(n)e^*(n) \mid d(n), \mathbf{w}(n)\}]$

$$= \boldsymbol{\eta} \cdot E[d(n)\theta_1^*(n)] + \frac{\mathbf{CM}(n)}{\sigma_z^2(n)} \cdot B_0$$, where

$B_0 = E\{\theta_3(n)\} - p(n) \cdot E\{d(n)\theta_1^*(n)\}$.

Consequently,

$$E\{y_k(n)e^*(n)\} = \eta_k \cdot E[d(n)\theta_1^*(n)] + \frac{[\mathbf{CM}(n)]_k}{\sigma_z^2(n)} \cdot B_0$$, $k = 0, ..., N-1$. Similarly, based on the assumption (d) such that $\mathbf{w}(n)$ is independent of $y(n)$,

$$E\{w_k^*(n)y_k(n)e^*(n)\} = M_k^*(n) \cdot \eta_k \cdot E[d(n)\theta_1^*(n)] + \frac{E\{\Phi_k(n)w_k^*(n)\}}{\sigma_z^2(n)} \cdot B_0,$$

$k = 0, ..., N-1$, and

$$E\{|y_k(n)|^2 \cdot |e^*(n)|^2\} = B_1 + 2\,\mathrm{Re}\left\{\frac{[\mathbf{CM}(n)]_k \cdot \eta_k^*}{\sigma_z^2(n)} \cdot B_2\right\} + \frac{E\{|\Phi_k(n)|^2\}}{\sigma_z^4(n)} \cdot B_3,$$

$k = 0,...,N-1$, can be shown, where

$$B_1 = C_{kk}E\{\theta_2(n)\} + |\eta_k|^2 E\{|d(n)|^2 \cdot \theta_2(n)\} ,$$

$$B_2 = E\{d^*(n)\theta_4(n)\} - p(n) \cdot E\{|d(n)|^2 \cdot \theta_2(n)\} , \text{ and}$$

$$B_3 = E\{\theta_5(n)\} - 2\,\mathrm{Re}[p^*(n)E\{d^*(n)\theta_4(n)\}] + |p(n)|^2 \cdot E\{|d(n)|^2 \cdot \theta(n)_2\} - \sigma_z^2 E\{\theta_2(n)\}$$

in which $\theta_2(n) = E\{|e^*(n)|^2 \mid d(n), \mathbf{w}(n)\}$, $\theta_4(n) = E\{z(n)|e(n)|^2 \mid d(n), \mathbf{w}(n)\}$ and $\theta_5(n) = E\{|z(n)|^2|e(n)|^2 \mid d(n), \mathbf{w}(n)\}$. Notably, $\theta_i(n)$, where $i = 1, 2, 3, 4, 5$ are functions of the random variable $d(n)$ and therefore are themselves random variables. Also, B_i, $i = 0, 1, 2, 3$ are all ensemble-average results for each iteration, n.

A. The MMA Output MSE Trajectory.

The MMA output MSE trajectory can be obtained from (4), (6), and (7) by setting $e(n)$ in (6) and (7) to $e_m(n) = e_{m,R}(n) + j \cdot e_{m,I}(n)$. Now, $\theta_i(n)$, where $i = 1, 2, 3, 4, 5$ can be determined based on assumption (b), such that $z(n) = z_R(n) + jz_I(n)$ conditioned on both $d(n)$ and $\mathbf{w}(n)$ is allowed to be a Gaussian random variable with mean and variance given by $E[z(n) \mid d(n), \mathbf{w}(n)] = \mu_z(n) = E[z_R(n) \mid d(n), \mathbf{w}(n)] + j \cdot E[z_I(n) \mid d(n), \mathbf{w}(n)] = \mu_R(n) + j\mu_I(n)$ and

$$VAR[z_R(n) \mid d(n), \mathbf{w}(n)] = VAR[z_I(n) \mid d(n), \mathbf{w}(n)] = \frac{1}{2}VAR[z(n) \mid d(n), \mathbf{w}(n)] = \frac{1}{2}\sigma_z^2(n) = \sigma^2(n)$$

, respectively, where $\mu_z(n)$ can be computed using $\mu_z(n) = d(n)p(n)$, and $VAR\{z(n) \mid d(n), \mathbf{w}(n)\} = \sigma_z^2(n)$ can be computed to be

$$\sigma_z^2(n) = \sum_{k=0}^{N-1}\Gamma_k(n)\lambda_k - E\{|d(n)|^2\}|\mathbf{M}^H(n)\boldsymbol{\eta}|^2 + E\{|d(n)|^2\} \cdot \sum_{i=0}^{N-1}(\Gamma_i(n) - |M_i(n)|^2)|\eta_k|^2 \quad [7].$$

Consequently, $\theta_1(n) \equiv E\{e_m(n) \mid d(n), \mathbf{w}(n)\}$ can be computed to be

$$\theta_1(n) \equiv E\{e_m(n) \mid d(n), \mathbf{w}(n)\}$$

$$= E[z_R(n) \cdot (z_R^3(n) - R_2) \mid d(n), \mathbf{w}(n)] + jE[z_I(n) \cdot (z_I^3(n) - R_2) \mid d(n), \mathbf{w}(n)]$$

$$= \int_{-\infty}^{\infty}[z_R^3(n) - z_R(n)R_2]\frac{1}{\sqrt{2\pi}\sigma(n)}\exp\{-\frac{[z_R(n) - \mu_R(n)]^2}{2\sigma^2(n)}\}dz_R(n) + j \cdot \int_{-\infty}^{\infty}[z_I^3(n) - z_I(n)R_2]\frac{1}{\sqrt{2\pi}\sigma(n)}\exp\{-\frac{[z_I(n) - \mu_I(n)]^2}{2\sigma^2(n)}\}dz_I(n)$$

$$= [\mu_R^3(n) + (3\sigma^2(n) - R_2)\mu_R(n)] + j[\mu_I^3(n) + (3\sigma^2(n) - R_2)\mu_I(n)]$$

Computation of $\theta_i(n)$ for $i = 2, 3, 4, 5$ can be computed similarly, yielding the results summarized in Table II.

B. The MSG-DDA Output MSE Trajectory

The MSG-DDA output MSE can be obtained from (4), (6), and (7) by setting $e(n)$ in (6) and (7) to $e_{msg}(n) = e_{msg,R}(n) + je_{msg,I}(n)$, where $e_{msg,R}(n) \equiv s[z_R(n)]$ and $e_{msg,I}(n) \equiv s[z_I(n)]$, as depicted in Table I. $\theta_i(n)$ for $i = 1, 2, 3, 4, 5$ must be evaluated to derive the output MSE trajectory in (4) for the MSG-DDA. For example, $\theta_1(n)$ can be computed to be

$$\theta_1(n) = E\{e_{msg}(n) \mid d(n), \mathbf{w}(n)\}$$
$$\equiv E\{e_{msg,R}(n) \mid d(n), \mathbf{w}(n)\} + jE\{e_{msg,I}(n) \mid d(n), \mathbf{w}(n)\}$$

Using Table I yields $\theta_1(n)$

$$= G_R^{01}(-\infty,-3,-3) + G_R^{01}(-\sqrt{8.2},-2,-3) + G_R^{01}(-1,0,-1) + G_R^{01}(0,1,1) + G_R^{01}(2,\sqrt{8.2},3) + G_R^{01}(3,\infty,3) + j[G_I^{01}(-\infty,-3,-3) + G_I^{01}(-\sqrt{8.2},-2,-3) + G_I^{01}(-1,0,-1) + G_I^{01}(0,1,1) + G_I^{01}(2,\sqrt{8.2},3) + G_I^{01}(3,\infty,3)]$$

where

$$G_R^{ij}(a,b,c) = \int_a^b z_R^i(n)[z_R(n) - c]^j \frac{1}{\sqrt{2\pi}\sigma(n)}\exp\{-\frac{[z_R(n) - \mu_R(n)]^2}{2\sigma^2(n)}\}dz_R(n)$$

and

$$G_I^{ij}(a,b,c) = \int_a^b z_I^i(n)[z_I(n) - c]^j \frac{1}{\sqrt{2\pi}\sigma(n)}\exp\{-\frac{[z_I(n) - \mu_I(n)]^2}{2\sigma^2(n)}\}dz_I(n)$$

$\theta_i(n)$ for $i = 2, 3, 4, 5$ can be computed similarly, yielding results summarized in Table III. The $G_R^{ij}(a,b,c)$ and $G_I^{ij}(a,b,c)$, can be expressed in terms of $F_n(x,y)$, n = 0,...,4, where $F_0(x,y) = Q(x) - Q(y)$, in which $Q(.)$ is the standard Q-function, defined as $Q(x) \equiv \int_x^\infty \frac{1}{\sqrt{2\pi}}\exp\{-\frac{t^2}{2}\}dt$, $F_1(x,y) = \frac{1}{\sqrt{2\pi}}(e^{-\frac{x^2}{2}} - e^{-\frac{y^2}{2}})$ and for $n \geq 2$,

$$F_n(x,y) = \frac{1}{\sqrt{2\pi}}(x^{n-1}e^{-\frac{x^2}{2}} - y^{n-1}e^{-\frac{y^2}{2}}) + (n-1)F_{n-2}(x,y) \quad .$$

(See [7].) Table IV gives expressions for $G_R^{ij}(a,b,c)$ and $G_I^{ij}(a,b,c)$.

III. SIMULATED VERIFICATION OF MSE ANALYSIS

This section demonstrates that the proposed MSG-DDA indeed considerably outperform both the MMA and the SGA for a 16-QAM square constellation, in terms of both the rate of convergence and the steady-state MSE. As depicted in Fig. 1, the transmitted data symbols $a(n)$ are an i.i.d. 16-QAM sequence, and the real and imaginary parts of the complex-valued additive white Gaussian noise $v(n)$ are assumed to be independent with equal variance such that the average signal noise ratio (SNR) is 40 dB. Figure 2 presents the impulse response of Channel A. The simulation described herein employed a complex equalizer with a transversal filter structure having 11 tap weights. The tap weights were initialized by setting the central tap weight to one, and the others to zero, denoted by $\mathbf{c}(0)$. According to this initial tap assignment, the first and the second moments

of the transformed tap coefficients were initialized as $\mathbf{M}(0) = \mathbf{U}\mathbf{c}(0)$ and $\Gamma_k(0) = |\mathbf{M}_k(0)|^2, k = 0,1,\ldots,N-1$. The overall delay of the channel and the equalizer is extended by padding with zeros such that the number of channel impulse responses equals the number of tap weights, which is 11; $N = 2L + 1 = 11$. Notably, the energy of the 16 QAM data constellation was normalized such that $E\{|d(n)|^2\} = 1$. The analytically computed MSE trajectories of the SGA (determined by judging whether the sign of the DD error is that of a Sato-like error analyzed in [7]), the MSG-DDA, and the MMA for Channel A are depicted in Fig. 3. The MSG-DDA indeed markedly outperforms the other two algorithms because the MSG-DDA determines whether it adapts its coefficients based on very tight bounds (much tighter than those used in the SGA analyzed in [7]) as presented in Table I. These strict conditions depicted in Table I tend to increase the reliability of the MSG-DDA and thus substantially increase its rate of convergence. Figure 4 depicts the simulated and analytically computed MSE trajectories of both the MSG-DDA and the MMA. The MSE trajectories predicted by the analyses agree with the simulation results very closely. Moreover, the accuracy of the analysis does not decline when the channel rotates the constellation.

Acknowledgement

This work was supported by the National Science Council (NSC), Taiwan, R.O.C. under contract NSC 92-2213-E-030-009.

References

[1] K. N. Oh and Y. O. Chin, "Modified constant modulus algorithm: blind equalization and carrier phase recovery algorithm," *Proc. 1995 IEEE Int. Conf. Commun.*, vol. 1, pp. 498-502.

[2] J. Yang, J.-J. Werner, and G. A. Dumont, "The multimodulus blind equalization and its generalized algorithms," IEEE Journal on Selected Areas in Communications, vol. 20, no. 5, pp. 997-1015, June 2002.

[3] Kun-Da Tsai and Jenq-Tay Yuan, "A Modified Constant and Carrier Recovery in Two-Dimensional Digital Communication Systems," *Seventh International Symposium on Signal Processing and its Applications (ISSPA 2003)*, pp. 563-566.

[4] G. Picchi and G. Prati, "Blind Equalization and Carrier Recovery Using a "Stop-and-Go" Decision-Directed Algorithm." *IEEE Trans. Commun.*, vol. COM-35, pp.877-887, Sept. 1987.

[5] D. Hatzinakos, "Blind Equalization Using Stop-and-go Adaptation Rules," Optical Engineering, vol. 31, no. 6, pp. 1181-1188, June 1992.

[6] V. Weerackody, S. A. Kassam, and K. R. Laker, "Convergence analysis of an algorithm for blind equalization," *IEEE Trans. Commun.*, vol. 39, pp. 856-865, June 1991.

[7] W. Lee and K. Cheun, "Convergence Analysis of the Stop-and-Go Blind Equalization Algorithm," *IEEE Trans. Commun.*, vol. 47, pp. 177-180, Feb. 1999.

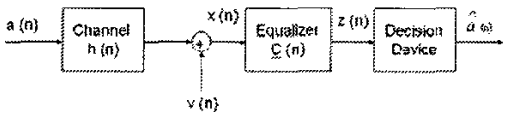

Fig. 1. Baseband model

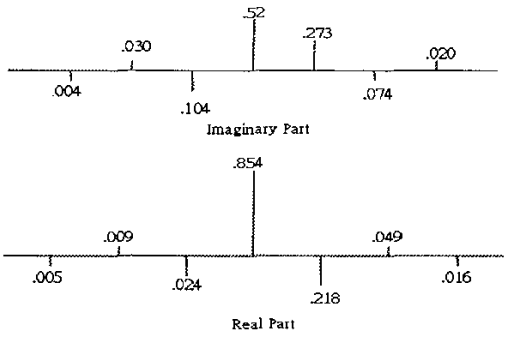

Fig. 2. Impulse response of Channel A

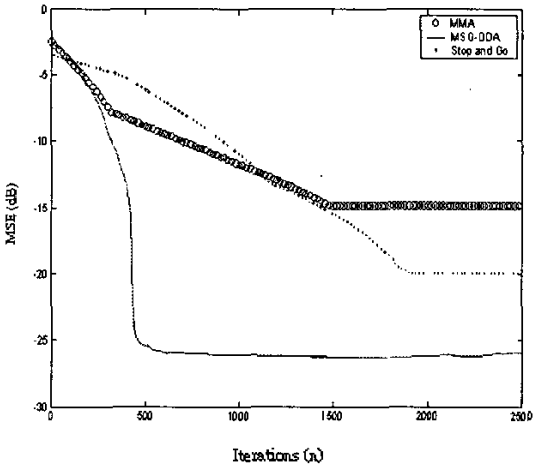

Fig. 3. The analytically computed MSE trajectories of MMA, SGA, and MSG-DDA

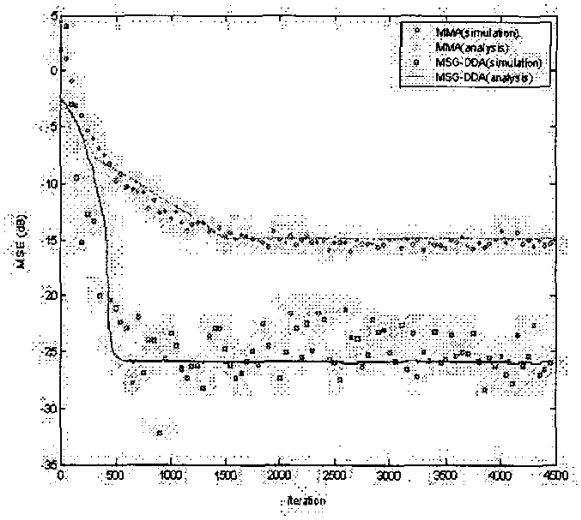

Fig. 4. Simulated and analytically computed MSE trajectories

Table I

MSG-DDA ERROR FOR SQUARE 16-QAM DATA CONSTELLATION

WITH DATA LEVELS AT ± 1 AND ± 3

$x = z_R(n)$ *or* $x = z_I(n)$

Conditions	s(x)
$x \le -2$ *and* $\operatorname{sgn}(x(x^2-8.2)) = \operatorname{sgn}(x+3)$ [*i.e,* $x \le -3$ *or* $-\sqrt{8.2} \le x \le -2$]	$x+3$
$-2 < x \le 0$ *and* $\operatorname{sgn}(x(x^2-8.2)) = \operatorname{sgn}(x+1)$ [*i.e,* $-1 \le x \le 0$]	$x+1$
$0 < x \le 2$ *and* $\operatorname{sgn}(x(x^2-8.2)) = \operatorname{sgn}(x-1)$ [*i.e,* $0 < x < 1$]	$x-1$
$x \ge 2$ *and* $\operatorname{sgn}(x(x^2-8.2)) = \operatorname{sgn}(x-3)$ [*i.e,* $x \ge 3$ *or* $2 \le x \le \sqrt{8.2}$]	$x-3$

Table II

COMPUTATION OF $\theta_i(n)$ *for* $i = 1,2,3,4,5$ FOR MMA

$$\theta_1(n) = [\mu_R^1(n) + (3\sigma^2(n) - R_2)\mu_R(n)] + j[\mu_I^1(n) + (3\sigma^2(n) - R_2)\mu_I(n)]$$

$$\theta_2(n) = [\mu_R^6(n) + (15\sigma^2(n) - 2R_2)\mu_R^4(n) + (45\sigma^4(n) - 12R_2\sigma^2(n) + R_2^2)\mu_R^2(n) + 15\sigma^6(n) - 6R_2\sigma^4(n) + R_2^2\sigma^2(n)] + [\mu_I^6(n) + (15\sigma^2(n) - 2R_2)\mu_I^4(n) + (45\sigma^4(n) - 12R_2\sigma^2(n) + R_2^2)\mu_I^2(n) + 15\sigma^6(n) - 6R_2\sigma^4(n) + R_2^2\sigma^2(n)]$$

$$\theta_3(n) = [(\mu_R^4(n) + \mu_I^4(n)) + (6\sigma^2(n) - R_2)(\mu_R^2(n) + \mu_I^2(n)) + 6\sigma^4(n) - 2R_2\sigma^2(n)] + j[\mu_R^3(n)\mu_I(n) - \mu_I^3(n)\mu_R(n)]$$

$$\theta_4(n) = [(\mu_R^7(n) + j\mu_I^7(n)) + (21\sigma^2(n) - 2R_2)(\mu_R^5(n) + j\mu_I^5(n)) + (105\sigma^4(n) - 20R_2\sigma^2(n) + R_2^2)(\mu_R^3(n) + j\mu_I^3(n)) + (105\sigma^6(n) - 30R_2\sigma^4(n) + 3R_2^2\sigma^2(n))(\mu_R(n) + j\mu_I(n))] + [(\mu_R(n)\mu_I^6(n) + j\mu_I(n)\mu_R^6(n)) + (15\sigma^2(n) - 2R_2)(\mu_R(n)\mu_I^4(n) + j\mu_R^4(n)\mu_I(n)) + (45\sigma^4(n) - 12R_2\sigma^2(n) + R_2^2)(\mu_R(n)\mu_I^2(n) + j\mu_I(n)\mu_R^2(n)) + (15\sigma^6(n) - 6R_2\sigma^4(n) + R_2^2\sigma^2(n))(\mu_R(n) + j\mu_I(n))]$$

$$\theta_5(n) = [(\mu_R^8(n) + \mu_I^8(n)) + (28\sigma^6(n) - 2R_2)(\mu_R^6(n) + \mu_I^6(n)) + (210\sigma^4(n) - 30R_2\sigma^2(n) + R_2^2)(\mu_R^4(n) + \mu_I^4(n)) + (420\sigma^6(n) - 90R_2\sigma^4(n) + 6R_2^2\sigma^2(n))(\mu_R^2(n) + \mu_I^2(n)) + (210\sigma^8(n) - 60R_2\sigma^6(n) + 6R_2^2\sigma^4(n))] + [(\mu_R^2(n)\mu_I^6(n) + \mu_I^2(n)\mu_R^6(n)) + (15\sigma^2(n) - 2R_2)(\mu_R^2(n)\mu_I^4(n) + \mu_I^2(n)\mu_R^4(n)) + (45\sigma^4(n) - 12R_2\sigma^2(n) + R_2^2)(\mu_R^2(n)\mu_I^2(n) + 2(15\sigma^6(n) - 6R_2\sigma^4(n) + R_2^2\sigma^2(n))(\mu_R^2(n) + \mu_I^2(n))] + [\sigma^2(n)(\mu_R^6(n) + \mu_I^6(n)) + (15\sigma^4(n) - 2R_2\sigma^2(n))(\mu_R^4(n) + \mu_I^4(n)) + (45\sigma^6(n) - 12R_2\sigma^4(n) + R_2^2\sigma^2(n))(\mu_R^2(n) + \mu_I^2(n)) + (30\sigma^8(n) - 12R_2\sigma^6(n) + 2R_2^2\sigma^4(n))]$$

Table III

COMPUTATION OF $\theta_i(n)$ *for* $i = 1,2,3,4,5$ FOR MSG-DDA

$$\theta_1(n) = [G_R^{01}(-\infty,-3,-3) + G_R^{01}(-\sqrt{8.2},-2,-3) + G_R^{01}(-1,0,-1) + G_R^{01}(0,1,1) + G_R^{01}(2,\sqrt{8.2},3) + G_R^{01}(3,\infty,3)] + j[G_I^{01}(-\infty,-3,-3) + G_I^{01}(-\sqrt{8.2},-2,-3) + G_I^{01}(-1,0,-1) + G_I^{01}(0,1,1) + G_I^{01}(2,\sqrt{8.2},3) + G_I^{01}(3,\infty,3)]$$

$$\theta_2(n) = [G_R^{02}(-\infty,-3,-3) + G_R^{02}(-\sqrt{8.2},-2,-3) + G_R^{02}(-1,0,-1) + G_R^{02}(0,1,1) + G_R^{02}(2,\sqrt{8.2},3) + G_R^{02}(3,\infty,3)] + [G_I^{02}(-\infty,-3,-3) + G_I^{02}(-\sqrt{8.2},-2,-3) + G_I^{02}(-1,0,-1) + G_I^{02}(0,1,1) + G_I^{02}(2,\sqrt{8.2},3) + G_I^{02}(3,\infty,3)]$$

$$\theta_3(n) = [G_R^{11}(-\infty,-3,-3) + G_R^{11}(-\sqrt{8.2},-2,-3) + G_R^{11}(-1,0,-1) + G_R^{11}(0,1,1) + G_R^{11}(2,\sqrt{8.2},3) + G_R^{11}(3,\infty,3)] + [G_I^{11}(-\infty,-3,-3) + G_I^{11}(-\sqrt{8.2},-2,-3) + G_I^{11}(-1,0,-1) + G_I^{11}(0,1,1) + G_I^{11}(2,\sqrt{8.2},3) + G_I^{11}(3,\infty,3)] + j\mu_I(n)[G_R^{01}(-\infty,-3,-3) + G_R^{01}(-\sqrt{8.2},-2,-3) + G_R^{01}(-1,0,-1) + G_R^{01}(0,1,1) + G_R^{01}(2,\sqrt{8.2},3) + G_R^{01}(3,\infty,3)] - j\mu_R(n)[G_I^{01}(-\infty,-3,-3) + G_I^{01}(-\sqrt{8.2},-2,-3) + G_I^{01}(-1,0,-1) + G_I^{01}(0,1,1) + G_I^{01}(2,\sqrt{8.2},3) + G_I^{01}(3,\infty,3)]$$

$$\theta_4(n) = [G_R^{12}(-\infty,-3,-3) + G_R^{12}(-\sqrt{8.2},-2,-3) + G_R^{12}(-1,0,-1) + G_R^{12}(0,1,1) + G_R^{12}(2,\sqrt{8.2},3) + G_R^{12}(3,\infty,3)] + \mu_R(n)[G_I^{02}(-\infty,-3,-3) + G_I^{02}(-\sqrt{8.2},-2,-3) + G_I^{02}(-1,0,-1) + G_I^{02}(0,1,1) + G_I^{02}(2,\sqrt{8.2},3) + G_I^{02}(3,\infty,3)] + j\mu_I(n)[G_R^{02}(-\infty,-3,-3) + G_R^{02}(-\sqrt{8.2},-2,-3) + G_R^{02}(-1,0,-1) + G_R^{02}(0,1,1) + G_R^{02}(2,\sqrt{8.2},3) + G_R^{02}(3,\infty,3)] + j[G_I^{12}(-\infty,-3,-3) + G_I^{12}(-\sqrt{8.2},-2,-3) + G_I^{12}(-1,0,-1) + G_I^{12}(0,1,1) + G_I^{12}(2,\sqrt{8.2},3) + G_I^{12}(3,\infty,3)]$$

$$\theta_5(n) = [G_R^{22}(-\infty,-3,-3) + G_R^{22}(-\sqrt{8.2},-2,-3) + G_R^{22}(-1,0,-1) + G_R^{22}(0,1,1) + G_R^{22}(2,\sqrt{8.2},3) + G_R^{22}(3,\infty,3)] + [G_I^{22}(-\infty,-3,-3) + G_I^{22}(-\sqrt{8.2},-2,-3) + G_I^{22}(-1,0,-1) + G_I^{22}(0,1,1) + G_I^{22}(2,\sqrt{8.2},3) + G_I^{22}(3,\infty,3)] + (\sigma^2(n) + \mu_R^2(n))[G_I^{02}(-\infty,-3,-3) + G_I^{02}(-\sqrt{8.2},-2,-3) + G_I^{02}(-1,0,-1) + G_I^{02}(0,1,1) + G_I^{02}(2,\sqrt{8.2},3) + G_I^{02}(3,\infty,3)] + (\sigma^2(n) + \mu_I^2(n))[G_R^{02}(-\infty,-3,-3) + G_R^{02}(-\sqrt{8.2},-2,-3) + G_R^{02}(-1,0,-1) + G_R^{02}(0,1,1) + G_R^{02}(2,\sqrt{8.2},3) + G_R^{02}(3,\infty,3)]$$

Table IV

EXPRESSIONS FOR $G_r^{ij}(a,b,c)$ *for* $r = R$ *or* I, *where* $a_r(n) = \dfrac{a-\mu_r(n)}{\sigma(n)}$ *and* $b_r(n) = \dfrac{b-\mu_r(n)}{\sigma(n)}$

$$G_r^{01}(a,b,c) = \sigma(n)F_1(a_r(n),b_r(n)) + (\mu_r(n) - c)F_0(a_r(n),b_r(n))$$

$$G_r^{11}(a,b,c) = \sigma^2(n)F_2(a_r(n),b_r(n)) + (2\mu_r(n) - c)\sigma(n)F_1(a_r(n),b_r(n)) + (\mu_r(n) - c)\mu_r(n)F_0(a_r(n),b_r(n))$$

$$G_r^{02}(a,b,c) = \sigma^2(n)F_2(a_r(n),b_r(n)) + 2\sigma(n)(\mu_r(n) - c)F_1(a_r(n),b_r(n)) + (\mu_r(n) - c)^2F_0(a_r(n),b_r(n))$$

$$G_r^{12}(a,b,c) = \sigma^3(n)F_3(a_r(n),b_r(n)) + (3\mu_r(n) - 2c)\sigma^2(n)F_2(a_r(n),b_r(n)) + \sigma(n)(\mu_r(n) - c)(3\mu_r(n) - c)F_1(a_r(n),b_r(n)) + \mu_r(n)(\mu_r(n) - c)^2F_0(a_r(n),b_r(n))$$

$$G_r^{22}(a,b,c) = \sigma^4(n)F_4(a_r(n),b_r(n)) + 2\sigma^3(n)(2\mu_r(n) - c)F_3(a_r(n),b_r(n)) + \sigma^2(n)(6\mu_r^2(n) - 6\mu_r(n)c + c^2)F_2(a_r(n),b_r(n)) + 2\sigma(n)\mu_r(n)(\mu_r(n) - c)(2\mu_r(n) - c)F_1(a_r(n),b_r(n)) + \mu_r^2(n)(\mu_r(n) - c)^2F_0(a_r(n),b_r(n))$$